JOURNAL OF MATERIALS SCIENCE **38** (2003) 2803–2807

# Investigation on the electrophoretic deposition of a FGM piezoelectric monomorph actuator

Y. H. CHEN, T. LI, J. MA
*School of Materials Engineering, Nanyang Technological University, Nanyang Avenue, Singapore 639798*
*E-mail: pg01185880@ntu.edu.sg*

In this paper, a FGM monomorph actuator was fabricated and its properties were also investigated. The procedure of fabricating such an actuator using electrophoretic deposition (EPD) was first established. The important processing parameters, such as zeta potential, were determined. The phase composition and microstructure of the deposits were examined using XRD and SEM. Smooth gradient microstructure was observed over the cross section and no significant defects and sharp interface was observed. The displacement of a monomorph, with dimension of 15.0 mm in length, 3.0 mm in width and 0.3 mm in thickness, was measured to be 4.16 $\mu$m under 100 V with low loss using photonic sensor. Both the microstructure and the electromechanical properties of the FGM monomorph actuator have indicated that EPD technique is a promising fabrication method for high performance components. 

## 1. Introduction

Piezoelectric ceramics such as lead zirconate-titanate (PZT) are widely used in applications such as actuators, transducers, and micropositioners [1]. Piezoelectric bimorphs are a typical type of piezoelectric device which can produce relatively large displacement [2]. They consist of two piezoelectric ceramic sheets which are bonded over their entire long faces and suitably covered with electrodes. Application of an external electric field across the piezoelectric sheets then results in a transverse deflection at the tip due to the axial contraction of one sheet and extension of the other sheet. However, it is noted that there exists severe disadvantages such as low reliability and poor interfacial bonding conditions in these layered structures. Thus, it is desirable to develop a monomorph with lower or no internal stress peaks when voltage is applied to and minimize structural discontinuity that can result in the failure of devices under cyclic loading. Recently, the concept of "Functionally Gradient" has been proposed to form monomorph [3–6]. Nevertheless, it is noted that the monomorphs proposed still exist sharp transitions due to limitations in the fabricating process.

In this report, a new FGM is proposed and the schematic structure is shown in Fig. 1. The proposed FGM actuator is designed to have a compositional gradient over the cross section. To achieve this, Electrophoretic deposition (EPD) technique was applied. EPD is a relatively new and effective method for the forming of functionally gradient and multilayer ceramic composites [7–9]. It is also observed that EPD technique is able to form both thick and thin smooth transition oxide components with complex shapes. Apart from the establishment of the fabrication procedures of the FGM monomorph actuator using EPD technique, the deposited component microstructural morphology and the bending displacement over a range of voltages are investigated.

## 2. Fabrication of FGM monomorph

In this section, the EPD process to form the FGM monomorphs with functionally gradients is described. The initial powders involve two kinds of PZT materials: $0.95Pb(Zr_{0.52}Ti_{0.48})O_3{\cdot}0.03BiFeO_3{\cdot}0.02Ba(Cu_{0.5}W_{0.5})O_3 + 0.5$ wt%$MnO_2$ (PZT1) and $Pb(Zr_{0.52}Ti_{0.48})O_3$ (PZT). The main advantage of selecting these two compositional materials is that they have similar sintering shrinkage at the same temperature.

Both PZT and PZT1 powders were prepared by conventional oxide mixing method. First, the raw oxide powders of PbO(>99.9%), $ZrO_2$(>99.9%), $TiO_2$(>99.9%), $Bi_2O_3$(>99.99%), $Fe_2O_3$(>99%), BaO(>99%), CuO(>99.99%), $WO_2$(>99%) and $MnO_2$(>99.99%) were weighed and mixed with the desired stoichiometrical composition. Considering the volatility of PbO during calcination and sintering, 3% excess of PbO was added into the raw powders. After ball milling for 24 h, the mixed oxides were calcined at 750°C and 800°C for 2 h for PZT1 and PZT respectively. Then, the calcined powders were smashed and ground by planetary ball milling at the speed of 150 rpm in ethanol for 20 h. Finally, the powders were passed through a 100-mesh sieve to remove the big agglomerations.

The particle size of PZT and PZT1 powders were then measured using an Acoustic Spectrometer DT-1200 (Dispersion Technology, Inc.) and confirmed by

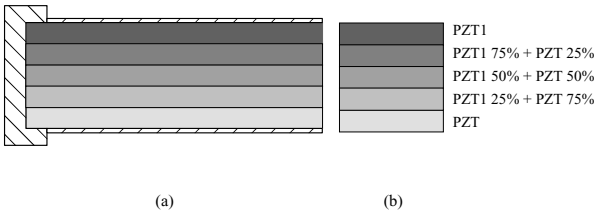


*Figure 1* Schematic structure of FGM monomorph actuator: (a) schematic structure and (b) composition profile of PZT-PZT1 FGM.

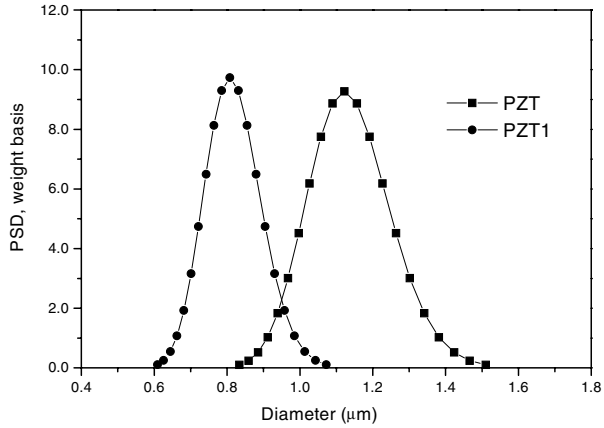


*Figure 2* Particle size distributions of PZT and PZT1 powders.

SEM observation. The distributions of particle size for both powders are shown in Fig. 2. The mean particle size of the PZT and PZT1 powders was noted to be 1.12 $\mu$m and 0.81 $\mu$m, respectively. The presence of particle size distributions in both powders can also be seen from the SEM images shown in Fig. 3. It is believed that such distribution improves the deposition density [10] as the smaller particles could insert into the pores formed between the bigger particles during deposition.

After measuring the particle size, the measurement of zeta potential was carried out using ZetaPlus (Brookhaven Instruments, USA). The measured zeta potential values at various pH are shown in Fig. 4. It is noted that the zeta potential of both suspensions reach maximum around pH 4.6, implying that both PZT and PZT1 are most stable at pH = 4.6, which is the desired condition for the EPD process.

Next, five suspensions for EPD were prepared by adding the prepared powders with composition as

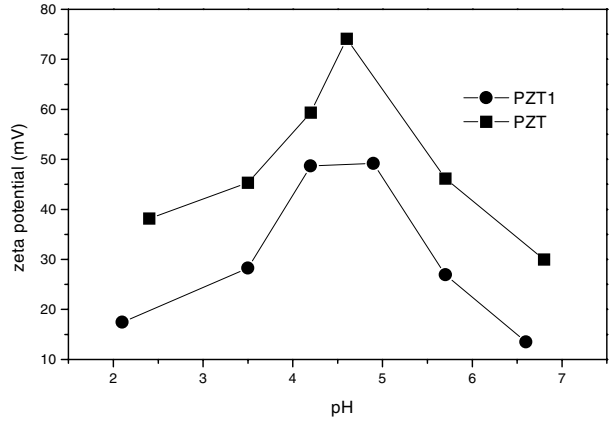


*Figure 4* Zeta potential vs. pH value of PZT and PZT1 suspensions.

shown in Fig. 1b in ethanol and then subjected to ultrasonic agitation for 10 min. The powder concentration in the suspension was 50 g/l and the suspension pH was controlled to be 4.6 by adding 10% $HNO_3$ at room temperature. The suspension was stirred for 3 to 6 h to make sure the complete dispersion of the powders in the medium.

The electrophoretic deposition system is schematically shown in Fig. 5. The electrophoretic cell includes a conductive foil as cathode and a stainless steel anode.

Multilayer deposition technique was adopted. The five suspensions described earlier were utilized for depositing consecutively in the designed order. Each suspension was deposited for 5 times, with each time last for 1 min. The interval between each deposition was controlled to be 10 min. The time control is important as otherwise the deposit will crack or peel off. The initial applied voltage was 25 V. The voltage was increased by 25 V each time when changing the suspension, since the resistance increases with the thickness of the deposits. After deposition, the deposits were dried in a dry keeper for 12 h.

The obtained FGM plates were sintered in a furnace at 1100°C for 1 h. They were then cut into rectangular-shaped piezoelectric plates and then coated with silver electrode and poled in silicone oil at 100°C for two hours under 2 kV/mm. After poling, the fabrication of the FGM piezoelectric monomorph actuator was completed.

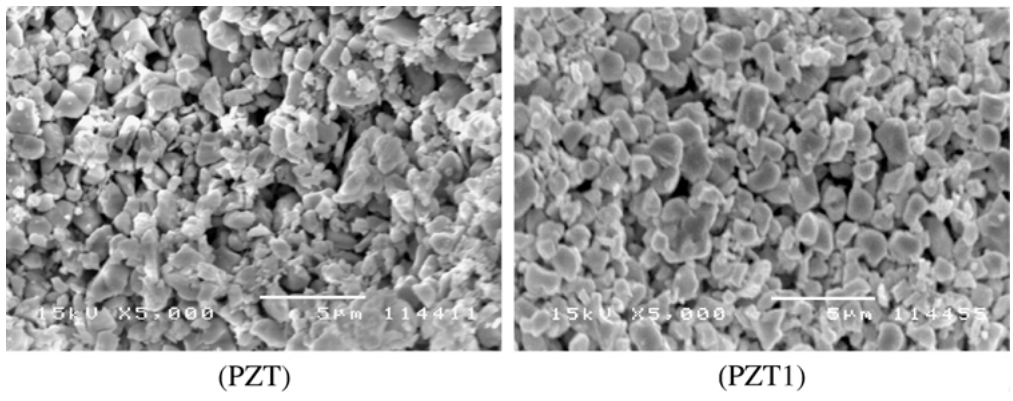


*Figure 3* SEM image of the PZT powders after deposition.

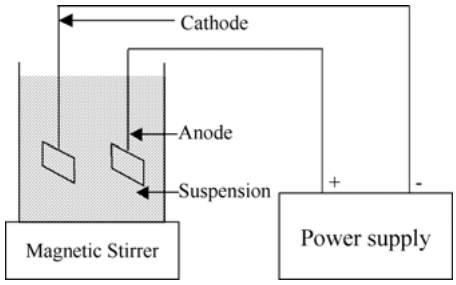


*Figure 5* Schematic drawing of electrophoretic deposition system.

## 3. Study of microstructure

In this section, the phase composition and microstructure of the deposits were examined using SEM and XRD.

The phase composition of the material in sintered plate was measured using XRD to ensure the formation of perovskite structure. Fig. 6 shows the XRD patterns of the materials. The single-phase perovskite structure was observed. From the small figure, it also can be determined that the materials is tetragonal phase [11]. The single tetragonal phase perovskite structure is the basis of FGM monomorph actuator to achieve good electromechanical performance.

Fig. 7a shows a cross section of the deposit observed using SEM. It can be seen that the structure is uniform and has even thickness. The experimental results shows that the thickness of the deposits after sintering can be as thin as 0.13 mm or as thick as 0.33 mm, which is difficult to be obtained by applying the normally FGM fabrication method such as tape casting, centrifugal casting or diffusion casting [5]. It can be also observed that no discrete interface and defects can be found, implying the good adhesion between each layer. This indicates that the current EPD technique can successfully produce miniaturized monomorph actuator with different size. Fig. 7b is a high magnification SEM micrograph. This area covers the gradient materials of 3 layers and the powders are observed to be homogeneously distributed.

Fig. 8 shows the cross section of the FGM plate after sintering at 1100°C. For this sample, the cross section has a thickness of approximately 0.27 mm measured from Fig. 8a. Over this cross section, the gradient change in microstructure can be observed. From the PZT side (left) to the PZT1 side (right), the grain size gradually increases. This is due to the compositional gradient over the cross section. Fig. 8b, c and d show the left, middle and right side of the cross section with higher magnification, respectively. The variation of piezoelectric properties over the cross section induced by compositional and microstructural gradient is the driving source to actuate the monomorph. The

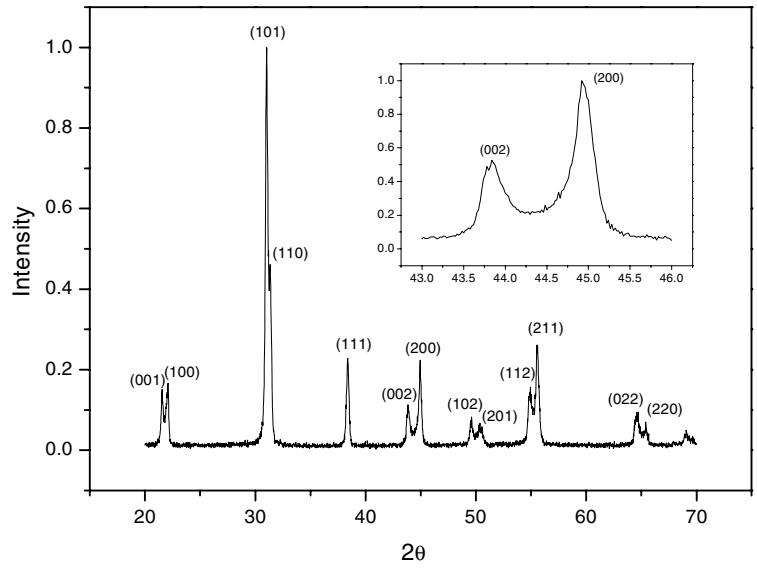


*Figure 6* XRD patterns of a FGM monomorph actuator sample.

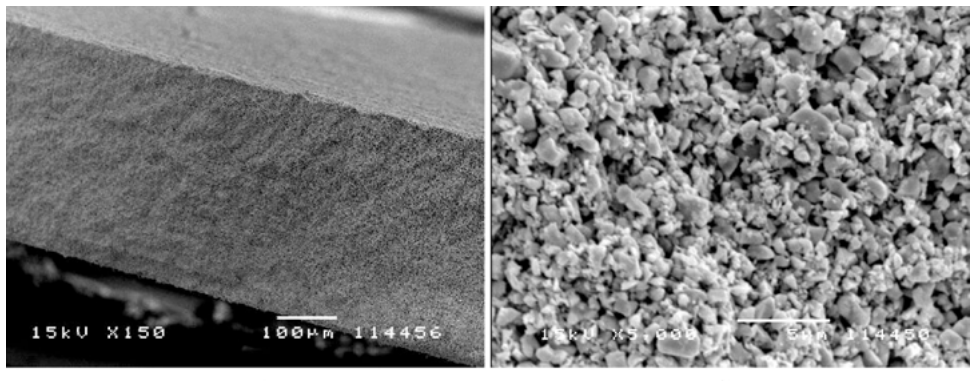


*Figure 7* Microstructure of the cross section of FGM deposit.

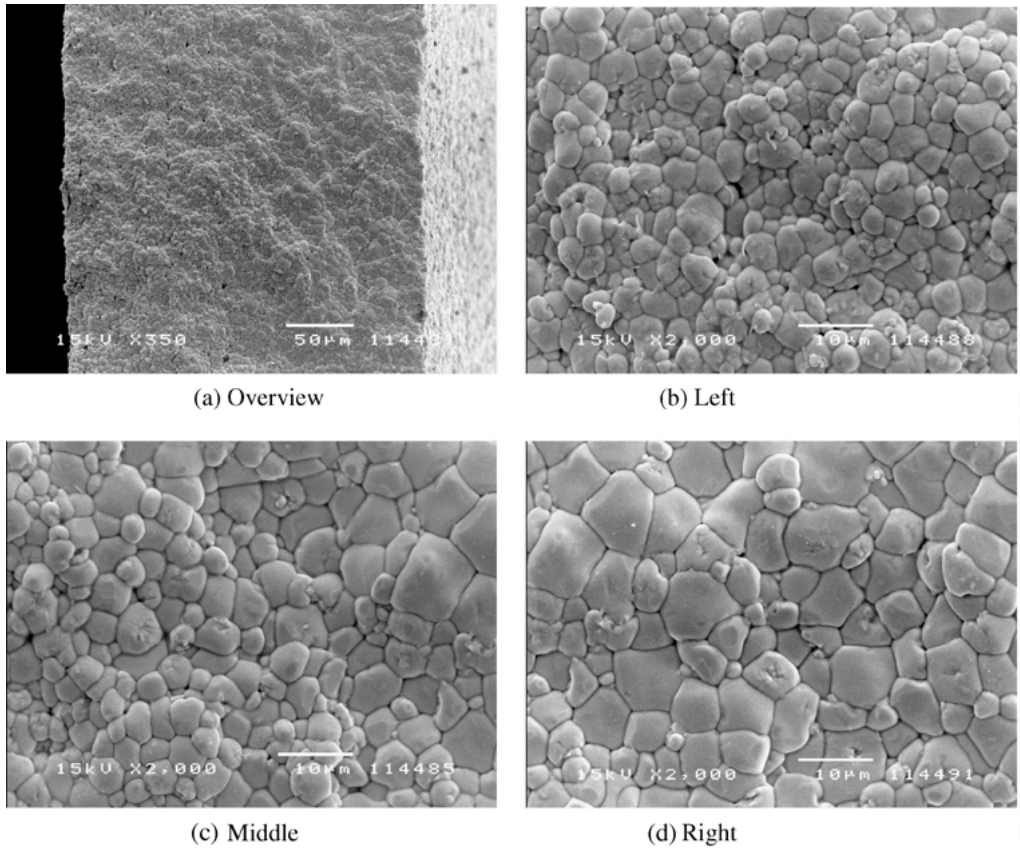


(a) Overview (b) Left

(c) Middle (d) Right

*Figure 8* Gradient variation of microstructure of FGM monomorph along cross section.

observed image in microstructure gradient also confirms the effectiveness of our procedure to fabricate FGM monomorph actuator.

## 4. Performance of FGM monomorph

In this section, one of the important parameters, bending displacement, of a fabricated FGM monomorph actuator was measured using a system consisting of RT6000HVS (Radiant Technologies, Inc.), a Vibraplane (RS Kinetic Systems, Inc.) and a MTI-2000 photonic sensor (probe: MTI2032RX. MTI Instruments). In the measurement, the monomorph was clamped to the vibraplane. A step voltage (0 to V to $-$V to 0) was applied to the monomorph via RT6000HVS. Then, the tip displacement of the monomorph at the free end was measured using the photonic sensor and the data was stored by the RT6000HVS.

The measured monomorph has a dimension of 15.0 mm in length, 3.0 mm in width and 0.3 mm in thickness. The hysteresis loop of the measured displacements versus applied voltage is shown in Fig. 9. A maximum displacement of 4.16 $\mu$m was obtained at applied voltage 100 V. It is also observed that the hysteresis of the loop is small indicating the good linear properties of the monomorph actuator and the low piezoelectric loss induced by the domain wall motion [12]. The displacement also suggests that the EPD prepared FGM monomorph can provide good electromechanically properties.

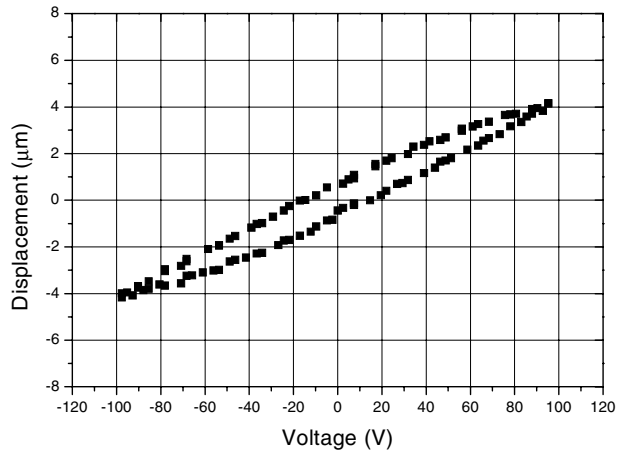


*Figure 9* Bending displacement of the FGM monomorph actuator in response to applied voltage.

## 5. Conclusions

EPD has been proven to be a good method to fabricate miniaturized FGM monomorph actuator via multilayer deposition technique. The obtained monomorph has a single-tetragonal-phase perovskite structure and fine gradient microstructure. No significant defects and very sharp interface can be observed over the cross section of the monomorph which is advantage in avoiding failures from internal debonding or from stress peaks developed in conventional bimorphs. The EPD prepared FGM monomorph provides good electromechanical properties with low loss.

## References

1. K. UCHINO, *MRS Bulletin* April 18 (1993) 42.
2. J. G. SMITS, S. I. DALKE and T. K. COONEY, *Sensors and Actuators* A **28** (1991) 41.

3. X. H. ZHU and Z. Y. MENG, *ibid.* A **48** (1995) 169.
4. CARL. C. M. WU, M. KAHN and W. MOY, *J. Amer. Ceram. Soc.* **79** (1996) 809.
5. W. F. SHELLEY, S. WAN and K. J. BOWMAN, *Mater. Sci. Foru.* **308–311** (1999) 515.
6. A. ALMAJID, M. TAYA and S. HUDNUT, *Int. J. Solids and Struct.* **38** (2001) 3377.
7. M. NAGAI, Y. YAMASHITA and Y. TAKUMA, *J. Amer. Ceram. Soc.* **76** (1993) 153.
8. B. FERRARI and R. MORENO, *J. Europ. Ceram. Soc.* **17** (1997) 549.
9. P. SARKAR, X. HUANG and P. S. NICHOLSON, *J. Amer. Ceram. Soc.* **75** (1992) 2907.
10. S. SUGIYAMA, A. TAKAGI and K. TSZUK, *J. Appl. Phys.* **30** (1991) 2170.
11. Y. YAMASHITA, *Jpn. J. Appl. Phys.* **33** (1994) 4652.
12. K. UCHINO and S. HIROSE, *IEEE Transactions on Ultrasonics, Ferroelectrics, and Frequency Control* **48** (2001) 307.

*Received 31 December 2002*
*and accepted 9 April 2003*